

Resonant Spheres: Multifrequency Detectors of Gravitational Waves

M. Angeles Serrano* and J. Alberto Lobo†

Departament de Física Fonamental, Universitat de Barcelona, Diagonal 647, 08028 Barcelona, Spain
(August 8, 2018)

We discuss the capabilities of spherical antennæ as single multifrequency detectors of gravitational waves. A first order theory allows us to evaluate the coupled spectrum and the resonators readouts when the first and the second quadrupole bare sphere frequencies are simultaneously selected for layout tuning. We stress the existence of non-tuning influences in the second mode coupling causing drags in the frequency splittings. These URF effects are relevant to a correct physical description of resonant spheres, still more if operating as multifrequency appliances like our PHCA proposal.

PACS numbers: 04.80.Nn, 95.55.Ym

A spherical antenna is particularly well adapted to sense metric tidal gravitational wave excitations as a consequence of the perfect matching between the GW radiation patterns and the sphere's vibration eigenmodes. When suitably monitored, it can act as an individual multimode detector generating potential knowledge on the incident direction of the signal, its quadrupole or monopole amplitudes, or its polarizations [1,2].

Spherical geometry also offers another substantial ability which optimizes the capabilities of resonant bars currently in operation [3]. By comparison, on equality of building material and mass, the estimated sphere's absorption cross section for the fundamental mode is over a factor of 4 better than that of a Weber's cylinder in its most favorable orientation. In addition, the second sphere's quadrupole still shows a rather large cross section, only about half its value at the lowest frequency and still about 15 times bigger than that associated to the cylinder for the fundamental mode, which is the only showing a significant cross section in bars [4]. Hence, *spheres show good sensitivity not only at the first but also at the second quadrupole harmonic, and therefore can efficiently operate at two frequencies as single multifrequency detectors.*

The challenge becomes how to take advantage of this potentiality. A preliminary task before multifrequency implementation design is to acquire a clear understanding of the detector's performance when working at one resonant frequency –see for instance [5] or [6].

The theories are proposed for practical multimode devices consisting of a perfect elastic sphere of radius R , mass M , density ρ and Lamé coefficients λ and μ , monitored by a suitable readout system, commonly a set of J identical resonators modelled as linear springs of mass $m \equiv \eta M, \eta \ll 1$, and endowed at certain positions $\mathbf{n}_a \equiv \mathbf{x}_a/R$ on the sphere's surface. Each resonator amplifies the elastic radial deformation $u_a(t)$ of the sphere at its attachment point caused by an external force and supplies an essential increase in the coupling by measuring the springs' deformations $q_a(t)$ rela-

tive to the sphere's undeformed surface. Resonant tuning requires the sensors to be typically built to possess a natural frequency Ω equal to one of the eigenfrequencies of the free sphere's spectrum, say ω_{NL} . This is always taken to be a monopole or a quadrupole frequency $-\omega_{N0}$ or ω_{N2} respectively, since only monopole or quadrupole sphere's spheroidal modes can be excited by an incoming wave [7].

In the universally assumed ideal approximation, the tuning frequency ω_{NL} is thought to be an isolated resonance frequency (IRF): no other frequency ω_{nl} of the free sphere's spectrum interferes in the resonance. For instance, this assumption is correct when the resonators couple to ω_{12} , in practice the most interesting coupling for unifrequency quadrupole radiation sensing [4].

We follow the perturbative approach in [6] naturally opened to refined analysis, and recall that the responses of the coupled device to an incident GW can be inferred from the system

$$\rho \frac{\partial^2 u_a}{\partial t^2} - \mu \nabla^2 u_a - (\lambda + \mu) \nabla(\nabla \cdot u_a) = \mathbf{f}_{res} + \mathbf{f}_{GW}$$

$$\ddot{q}_a(t) + \Omega_a^2 q_a(t) = -\ddot{u}_a(t) + \zeta_{a,GW}(t) \quad a = 1, \dots, J, \quad (1)$$

where $\mathbf{f}_{res}(x_a, t)$ and $\mathbf{f}_{GW}(x_a, t)$ are respectively due to the resonators' back action on the sphere and to the incident GW which also causes a tidal acceleration $\zeta_{a,GW}(t)$ on resonator a .

After implementation of Green function formalism, the equations can be rewritten in the s -Laplace domain as

$$\sum_{b=1}^J M_{ab} \hat{q}_b(s) = -\frac{s^2}{s^2 + \omega_{NL}^2} \hat{u}_{a,GW}(s) + \frac{\hat{\zeta}_{a,GW}(s)}{s^2 + \omega_{NL}^2},$$

$$a = 1, \dots, J, \quad (2)$$

with $\hat{u}_{a,GW}(s)$ the bare sphere's radial responses to the signal at the resonators' locations.

In the IRF circumstance, matrix M_{ab} is of the form

$$M_{ab} \equiv \left[\delta_{ab} + \eta \frac{s^2 \omega_{NL}^2}{s^2 + \omega_{NL}^2} P_{L,ab} \right]. \quad (3)$$

The geometric properties of a particular resonator arrangement are displayed by the $J \times J$ symmetric real matrix P_L associated to the L -mode selected for tuning. It basically has as element ab the Legendre polynomial of order L , a sum of products of spherical harmonics:

$$P_{L,ab} = |A_{NL}(R)|^2 \sum_{m=-L}^{m=L} Y_{LM}^*(\mathbf{n}_a) Y_{LM}(\mathbf{n}_b) \quad (4)$$

with $A_{NL}(R)$ radial components in the spheroidal normal modes of the free sphere [7]. It is highly remarkable that all the information determining the distinctive readout of a given configuration is just concentrated the eigenvalues ξ_a^2 and eigenvectors $v^{(a)}$ of P_L .

First order resolution for the spectrum of coupled-mode eigenfrequencies from $\det M_{ab} = 0$ shows that the attachment of resonators causes the tuning frequency ω_{NL} to split into J *symmetric pairs* around the original value,

$$\omega_{a,\pm}^2 = \omega_{NL}^2 \left(1 \pm \xi_a \eta^{\frac{1}{2}}\right) + O(\eta) \quad a = 1, \dots, J, \quad (5)$$

whereas resonators amplitudes amount to be linear combinations of the GW amplitudes $\hat{g}^{(2m)}(s)$:

$$\hat{g}_a(s) = \eta^{-\frac{1}{2}} \sum_{b=1}^J \sum_{\pm \xi_c \neq 0} \left\{ F_L(\pm \xi_c) \frac{1}{(s^2 + \omega_{c,\pm}^2)} v_a^{(c)} v_b^{(c)*} \right\} \times \left. \sum_{m=-2}^{m=2} Y_{2m}(\mathbf{n}_b) \hat{g}^{(2m)}(s) \right\} + O(0) \quad a = 1, \dots, J. \quad (6)$$

$$F_L(\pm \xi_c) = \pm [a_{NL} A_{NL}(R)] (-1)^J (\xi_c)^{-1}$$

with a_{NL} non zero overlap coefficients only if $L = 0$ or $L = 2$ [7].

Layout	IRF Eigenfrequencies	
	around ω_{12}	around ω_{22}
PHCA	$\omega_{0,\pm} = \omega_{12}(1 \pm 0.58\eta^{\frac{1}{2}})$	$\omega_{0,\pm} = \omega_{22}(1 \pm 0.03\eta^{\frac{1}{2}})$
	$\omega_{1,\pm} = \omega_{12}(1 \pm 0.88\eta^{\frac{1}{2}})$	$\omega_{1,\pm} = \omega_{22}(1 \pm 0.05\eta^{\frac{1}{2}})$
	$\omega_{2,\pm} = \omega_{12}(1 \pm 1.07\eta^{\frac{1}{2}})$	$\omega_{2,\pm} = \omega_{22}(1 \pm 0.06\eta^{\frac{1}{2}})$
TIGA	$\omega_{\pm} = \omega_{12}(1 \pm 1.00\eta^{\frac{1}{2}})$	$\omega_{\pm} = \omega_{22}(1 \pm 0.05\eta^{\frac{1}{2}})$

TABLE I. IRF frequencies around ω_{12} and ω_{22} for the PHCA and TIGA arrangements.

However, this is not always the case that the interesting frequency for tuning is an isolated resonant frequency. For example, the second quadrupole ω_{22} is in

fact a suitable sphere's frequency for a second resonator set to be tuned in order to exploit the antenna as a multifrequency device. A careful examination of the spectrum of a typical planned full scale aluminium sphere $-\eta_s \approx 1/40000$, $R = 1.5m$ — around ω_{22} shows that ω_{14} is merely within a distance of order $\eta^{\frac{1}{2}}$:

$$\omega_{14}^2 = \omega_{22}^2 \left(1 + K \eta^{\frac{1}{2}}\right), \quad (7)$$

where the dimensionless parameter K takes the negative value $K = -2.21$ for $\eta = \eta_s$.

The expectation is that this nearness alters in some way the above IRF results. The effects of such unisolation –URF effects [8]– must be accurately considered to reach a faithful description of the detector's real behaviour.

Let us analyse the general case when ω_{NL} is the single selected frequency for tuning and $\omega_{N'L'}$ is in its neighbourhood. Again, we start from expressions (1) and (2) which remains unchanged, although a new contribution appears in (3):

$$M_{ab} \equiv \left[\delta_{ab} + \eta \frac{s^2 \omega_{NL}^2}{(s^2 + \omega_{NL}^2)^2} P_{L,ab} + \eta \frac{s^2 \omega_{N2}^2}{(s^2 + \omega_{N2}^2)(s^2 + \omega_{N'L'}^2)} P_{L',ab} \right]. \quad (8)$$

We can still go further in drawing generic conclusions valid for any resonator distribution whenever it allows P_L and $P_{L'}$ to commute: $[P_L, P_{L'}] = 0$. Then, we name $v^{(a)}$ the orthogonal basis which simultaneously diagonalises the two matrices, with eigenvalues $\xi_{a,L}^2$ and $\xi_{a,L'}^2$ respectively, so that in this basis M_{ab} is also diagonal. Then, the URF resonances around ω_{NL} can be written in J triplets

$$\omega_{a,T}^2 = \omega_{NL}^2 \left(1 + U_a^T \eta^{\frac{1}{2}}\right) + O(\eta) \quad a = 1, \dots, J, \quad (9)$$

where for each resonator index a , the upper label $\{T\}$ represents the group $\{u, c, d\}$ which refers to the three different solutions of the cubic equation

$$U_a^3 - K \cdot U_a^2 - \chi^2 \cdot U_a + K \xi_{a,2}^2 = 0 \quad \chi^2 = \xi_{a,2}^2 + \xi_{a,L'}^2, \quad (10)$$

with parameters which are univocally determined by fixing the layout, ω_{NL} and $\omega_{N'L'}$. Inspection of orders of magnitude in (10) for $\omega_{NL} = \omega_{22}$ and $\omega_{N'L'} = \omega_{14}$ leads to the conclusion that the triplets present a general pattern with independence of the resonator distribution: one of the three frequencies will always be located very close to the original tuning frequency ω_{22} –to assess how much near this frequency actually is one needs to restrict to particular cases and numerical evaluations–. The remaining pair forms a non-symmetric doublet around it,

in good agreement with the idea that the presence of ω_{14} causes a perturbation of the ideal IRF situation.

Then, the URF effect results in a dragging effect breaking the symmetry of the IRF doublets which approach the disturbing frequency ω_{14} , and moreover induces the appearance of a third central component near the resonant ω_{22} .

Near actually means really near, at least for two known proposals: PHCA [9,10] and TIGA [5,11]. It can be seen from the numbers in Table II that in each a-group the central U_a^c is itself of order $\eta^{\frac{1}{2}}$ or smaller, so that these central URF resonances actually differ from ω_{22} in terms of order η . Reproduction of the amplitudes evaluation process demonstrates that the contribution of such modes are not at leading order $\eta^{-\frac{1}{2}}$ but at higher terms. Therefore, they are referred to as be weakly coupled.

Layout	Strongly Coupled	Weakly Coupled
PHCA	$\omega_{0,u} = \omega_{22}(1 + 0.06\eta^{\frac{1}{2}})$ $\omega_{0,d} = \omega_{22}(1 - 1.16\eta^{\frac{1}{2}})$	$\omega_{0,c} = \omega_{22}(1 - 3.3 \cdot 10^{-3}\eta^{\frac{1}{2}})$
	$\omega_{1,u} = \omega_{22}(1 + 1.41\eta^{\frac{1}{2}})$ $\omega_{1,d} = \omega_{22}(1 - 2.51\eta^{\frac{1}{2}})$	$\omega_{1,c} = \omega_{22}(1 - 1.5 \cdot 10^{-4}\eta^{\frac{1}{2}})$
	$\omega_{2,u} = \omega_{22}(1 + 1.07\eta^{\frac{1}{2}})$ $\omega_{2,d} = \omega_{22}(1 - 2.18\eta^{\frac{1}{2}})$	$\omega_{2,c} = \omega_{22}(1 - 3.5 \cdot 10^{-4}\eta^{\frac{1}{2}})$
TIGA	$\omega_{1-5,u} = \omega_{22}(1 + 1.22\eta^{\frac{1}{2}})$ $\omega_{1-5,d} = \omega_{22}(1 - 2.32\eta^{\frac{1}{2}})$	$\omega_{1-5,c} = \omega_{22}(1 - 2.5 \cdot 10^{-4}\eta^{\frac{1}{2}})$
	$\omega_{6,S} = \omega_{22}(1 - 1.105\eta^{\frac{1}{2}})$	$\omega_{6,D} = \omega_{22}$

TABLE II. SCD+WCS URF triplets around ω_{22} . Calculation have been performed for the proposals PHCA and TIGA, and for η_s , a theoretical value for a full scale future spherical detector. Subindex u (up) labels the values which are above the resonance frequency ω_{22} , whereas d (down) labels those underneath, and c (central) those practically at ω_{22} .

The result is that both PHCA and TIGA URF triplets are composed of a weakly coupled singlet plus a strongly coupled doublet (triplet named of the SCD+WCS type) of span comparable to that of the IRF pairs. The only exception is the sixth mode in TIGA which corresponds to a triplet composed of a strongly coupled singlet plus a weakly coupled doublet (SCS+WCD type). Also, the degeneracy pattern of the IRF triplets is maintained: for PHCA, three different triplets, two of them doubly degenerated, and for TIGA one triplet five-fold degenerate plus one single weakly coupled triplet.

As said, only strongly coupled frequencies (SC) con-

tribute to the amplitudes:

$$\hat{q}_a(s) = \eta^{-\frac{1}{2}} \sum_{b=1}^J \sum_{SC} \left\{ F_{LL'}(U_c^{SC}) \frac{1}{(s^2 + \omega_{c,SC}^2)} v_a^{(c)} v_b^{(c)*} \right\} \times \sum_{m=-2}^{m=2} Y_{2m}(\mathbf{n}_b) \hat{g}^{(2m)}(s) + O(0) \quad a = 1, \dots, J, \quad (11)$$

with frequency weights

$$F_{LL'}(U_c^{SC}) = \left[a_{NL} A_{NL} + a_{N'L'} A_{N'L'} \frac{U_c^{SC}}{U_c^{SC} - K} \right] \times \frac{U_c^{SC} - K}{\prod_{SC' \neq SC''} (U_c^{SC'} - U_c^{SC})(U_c^{SC''} - U_c^{SC})}. \quad (12)$$

The high degree of symmetry showed by both PHCA and TIGA explains why these configurations fulfil the property $[P_L, P_{L'}] = 0$ for $L = 2$ and $L' = 4$, so that P_2 and P_4 simultaneously diagonalise. After algebraic calculus, the eigenvectors of the common basis are finally found to be arrangements of spherical harmonics of order two, precisely the eigenvectors of P_2 when diagonalised separately in the IRF situation:

$$v_a^{(m)} = \sqrt{\frac{4\pi}{5}} \xi_{m,(2)}^{-1} Y_{2m}(\mathbf{n}_a). \quad (13)$$

By inserting these functions in (12), we arrive to simplified expressions for the readouts of the PHCA layout:

$$\hat{q}_{a,PHCA}(s) = \eta^{-\frac{1}{2}} \sum_{SC} \left\{ F_{24}(U_0^{SC}) \frac{Y_{20}(\mathbf{n}_a) \hat{g}^{(20)}(s)}{(s^2 + \omega_{0,SC}^2)} + F_{24}(U_1^{SC}) \frac{[Y_{21}(\mathbf{n}_a) \hat{g}^{(21)}(s) + Y_{2-1}(\mathbf{n}_a) \hat{g}^{(2-1)}(s)]}{(s^2 + \omega_{1,SC}^2)} + F_{24}(U_2^{SC}) \frac{[Y_{22}(\mathbf{n}_a) \hat{g}^{(22)}(s) + Y_{2-2}(\mathbf{n}_a) \hat{g}^{(2-2)}(s)]}{(s^2 + \omega_{2,SC}^2)} \right\}; \quad (14)$$

and the readouts of the TIGA layout:

$$\hat{q}_{a,TIGA}(s) = \eta^{-\frac{1}{2}} \sum_{SC} F_{24}(U_{1-5}^{SC}) \frac{\sum_{m=2}^{m=2} Y_{2m}(\mathbf{n}_a) \hat{g}^{(2m)}(s)}{(s^2 + \omega_{1-5,SC}^2)}. \quad (15)$$

The weight functions $F_{24}(U_c)^{SC}$ in (14) and (15) can be settled from (12). It is here important to recall that the overlap coefficient a_{14} is zero, which is in accordance with the idea that only monopole or quadrupole sphere's modes can be excited by an impinging GW. One has to take also into account that just *up* and *down* frequencies in the triplets correspond to SC values, and that the the

remaining U_c^c give place to weakly coupled resonances which do not contribute at leading order. Hence,

$$F_{24}(U_c^{SC}) = F_{24}(U_c^{u,d}) = a_{22}A_{22} \frac{1}{U_c^{d,u} - U_c^{u,d}} \frac{U_c^{d,u}}{U_c^{u,d}}. \quad (16)$$

In Figure 1 we display numerical simulations for the IRF and URF qualitative responses caused by the action of a GW burst travelling down the symmetry axis of the PHCA pentagonal layout. In both cases the practical outputs become beats, although differing in modulation and modulated frequencies. The IRF output exactly cancels at the nodes because the weights affecting the contributions to the amplitudes of ω_+ and ω_- equal each other whereas the URF readout shows a certain thickness at those same points caused by the difference between the weights associated to ω_u and ω_d . The occurrence of different weights is in direct relation to the dragging induced by the URF effect which breaks the symmetry of the IRF-doublets. Nevertheless, the similarity of the patterns again corroborates the weakness of the new third central frequency in the URF triplets.

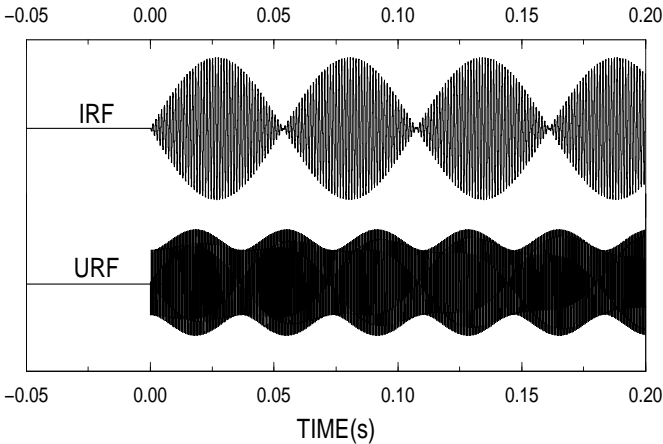


FIG. 1. PHCA beat outputs for GW burst with $h_+ = h_\times$ propagating along the pentagonal symmetry axis at $t=0$.

Hence, the analysis of the URF effect is essential for a complete study of any spherical multifrequency GW detector, but we are specially interested in it with respect to our PHCA proposal.

It is actually idealized as a multifrequency antenna with two sets of supplementary pentagonal layouts, one tuned to the first quadrupole harmonic ω_{12} and another coupled to the second quadrupole harmonic ω_{22} , which in fact has ω_{14} very close to it. The pentagonal hexacontahedron polyhedric shape with more than enough number of faces for 10 resonators matching in non parallel pentagonal positions (and even an eleventh resonator position for monopole sensing) guarantees technical feasibility, also supported by the absence of cross interactions between the outputs of each set at order $\eta^{-\frac{1}{2}}$. Our

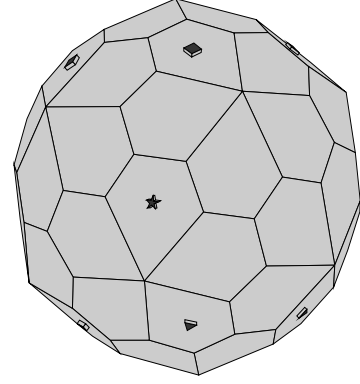


FIG. 2. PHCA Proposal. Marked faces in the pentagonal hexacontahedron indicate resonator positions: a *square* for transducers tuned to ω_{12} , a *triangle* for that tuned to ω_{22} , and a *star* for the monopole sensor.

model ensures a correct description of the multifrequency PHCA coupled spectrum. We find two main groups of frequencies, the first composed of pairs symmetrically distributed around ω_{12} and the second arising as a non-symmetrical splitting of ω_{22} in triplets dragged towards ω_{14} .

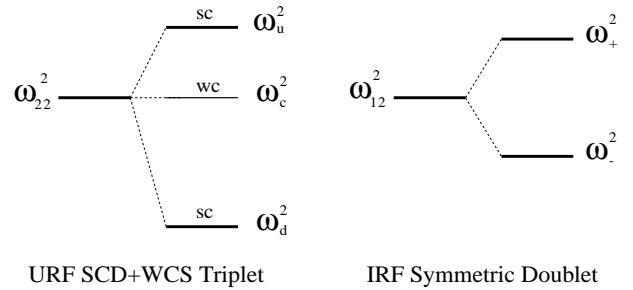


FIG. 3. PHCA multifrequency spectrum.

The PHCA monitored at their first two quadrupole modes can for instance be advantageously used to detect chirp signals from coalescing binary systems, and even to determine some of their characteristic parameters by means of a robust double passage method [12]. This potentiality, unthinkable for currently operating bars, shows that resonant spherical antennae are abreast of projected broadband large laser interferometers with respect to their predicted ability in monitoring gravitational waves from these sources [13].

In any case, the URF effect plays *per se* an essential part in a rigorous theoretical analysis of any single multifrequency GW detector. Its features are concisely reported by our developments without severely complicating the evaluations. We conclude by emphasizing that the philosophy underlying these algorithms is easily extensible to the study of other practical real situations

departing from ideality.

M. A. Serrano thanks Tomás Alarcón and Miquel Montero for active encouragement, and José M. Pozo for many helpful mathematical discussions. This research is supported by the Spanish Ministry of Education under grant No. FP97-46725209 and contract No. PB96-0384, and the Institut d'Estudis Catalans.

* E-mail address: marian@hermes.ffn.ub.es

† E-mail address: lobo@hermes.ffn.ub.es

- [1] Wagoner R.V. and Paik H.J., in *Proc. of the Int. Symp. on Exp. Grav.*, Academia Nazionale dei Lindei, Rome (1977).
- [2] Magalhães N. S. *et al.*, *Mon. Not. R. Astron. Soc.*, **274**, 670 (1995).
- [3] Coccia E. *et al.*, in *Proceedings of the GR-14 Conference*, World Scientific, Singapore (1997).
- [4] Coccia E., Lobo J.A. and Ortega J.A., *Phys. Rev. D*, **52**, 3735 (1995).
- [5] Johnson W.W. and Merkowitz S.M., *Phys. Rev. Lett.*, **70**, 2367 (1993).
- [6] Lobo J.A. and Serrano M.A., submitted to *Mon. Not. R. Astron. Soc.*, (astro-ph/9904198).
- [7] Lobo J.A., *Phys. Rev. D*, **52**, 591 (1995).
- [8] Serrano M.A, *PhD Thesis*, University of Barcelona (1999).
- [9] Lobo J.A. and Serrano M.A, *Europhys. Lett.*, **35**, 253 (1996).
- [10] Lobo J.A. and Serrano M.A, *Class. Quant. Grav.*, **14**, 1495 (1997).
- [11] Merkowitz S.M. and Johnson W.W., *Phys. Rev. D*, **51**, 2546 (1995).
- [12] Coccia E. and Fafone V., *Phys. Lett.*, **A213**, 16 (1996).
- [13] Krolak A., Lobo J.A. and Meers B.J., *Phys. Rev. D*, **43**, 2470 (1991).